Transdermal delivery of mitochondrial-targeted hydrogen sulphide donor, AP39 protects against 6-hydroxydopamine-induced mitochondrial dysfunction

Mandeep Kaur Marwah[1]*, Bahareh Manhoosh[1], Hala Shokr[2], Mohamad Anas Al Tahan[3], Roderick Stewart[4,5], Mohammed Iqbal[6], Lorena Diaz Sanchez[1], Sewa Abdullah[1], Shakil Ahmad[1], Keqing Wang[1], Karan Singh Rana[6], Lissette Sanchez-Aranguren[1]*

[1]Aston Medical School, College of Health and Life Sciences, Aston University, UK.

[2]Pharmacy Division, School of Health Sciences, Faculty of Biology, Medicine and Health, University of Manchester, UK.

[3]School of Pharmacy, College of Health and Life Sciences, Aston University, UK.

[4]Quest Healthcare, Birmingham, UK.

[5]Aston Pharmacy School, College of Health and Life Sciences, Aston University, UK.

[6]School of Biosciences, College of Health and Life Sciences, Aston University, UK.

***Correspondence:**

Dr. Lissette Sanchez-Aranguren. Email: l.sanchez-aranguren2@aston.ac.uk

ORCID ID: https://orcid.org/0000-0002-4663-5752

Dr. Mandeep Kaur Marwah. Email: m.marwah1@aston.ac.uk

ORCID ID: https://orcid.org/0000-0003-4881-003X

Abstract

Hydrogen sulphide (H_2S) is an important gaseous signalling molecule with emerging roles as a neuroprotectant. The objective of this study was to investigate the feasibility of transdermal delivery of mitochondrial-targeted H_2S donor, AP39 whilst investigating the ability of permeated AP39 on abrogating 6-hydroxydopamine (6-OH-dop)-induced mitochondrial dysfunction, as a model of Parkinson's disease, established in human neuroblastoma cells, SHSY-5Y. Aqueous hypromellose gels (5% w/v) were prepared with up to 10% v/v propylene glycol (PG) with 0.002% w/w AP39. AP39 permeation from formulations across excised murine skin into PBS was quantified over 24 h using HPLC-UV detection. Media was collected and applied to a microvasculature blood-brain-barrier (BBB) model to evidence AP39 permeability. Following, the permeate was applied to neuroblastoma cells SHSY-5Y to evidence its therapeutic potential in modulating the mitochondrial bioenergetics and

antioxidant in response to 6-OH-dop-induced mitochondrial dysfunction. The presence of PG in gel formulations significantly increased the cumulative amount of AP39 permeated across murine skin over 24 hours from 24.40 ± 2.39 % to 48.59 ± 2.93 %. Conditioned media applied to a microvasculature BBB model observed AP39 permeation across the barrier and H_2S release. Finally, permeated AP39 enhanced parameters of mitochondrial bioenergetics in SHSY-5Y exposed to 6-OH-dop. Moreover, permeated AP39 abrogated mitochondrial-specific reactive oxygen species generation induced by 6-OH-dop. These findings demonstrate transdermal delivery of AP39 may provide a promising alternative to deliver this mitochondrial-targeted H_2S donor and this approach allows the potential to cross the BBB reaching CNS organs in the treatment of neurodegenerative conditions such as Parkinson's disease. Moreover, our observations show that gels prepared with 10% v/v PG have the potential for use in conditions requiring rapid H_2S delivery whereas gels without PG for therapy requiring sustained H_2S delivery.

Keywords: transdermal drug delivery, sustained release, mitochondrial bioenergetics, neurodegenerative conditions, hydrogen sulphide donors.

1. Introduction

Parkinson's disease (PD) is a neurodegenerative disorder, associated with the loss of function of dopaminergic neurones in the substantia nigra (1). The resultant dysregulation of basal ganglia circuitries is responsible for the most prominent motor symptoms, including bradykinesia, hypokinesia, rigidity, resting tremor and postural instability (1). PD is associated with various pathophysiological processes, including mitochondrial dysfunction, oxidative stress and the accumulation of aberrant or misfolded proteins (2, 3). Treatments are limited in effectiveness, therefore, there is a pressing need to address this growing healthcare burden.

Hydrogen sulphide (H_2S) is an endogenous gaseous transmitter reported to serve many physiological and pathological functions in various tissues, including the central nervous system (4, 5) with novel emerging roles as a neuroprotectant. Within the mitochondria, H_2S donates electrons to the electron transport chain, therefore acting as an inorganic source of energy (6) whilst enhancing electron transport and mitochondrial bioenergetics (7). Recent evidence suggests that H_2S donors have potential therapeutic value against neurodegenerative disorders due to their ability to produce anti-oxidant, -inflammatory, and -apoptotic effects in pathological situations (8). Particularly, in a 6-hydroxydopamine (6-OH-dop)-induced PD model, a significant reduction in H_2S levels in the substantia nigra has been evidenced (9). Furthermore, the administration of H_2S donors have shown to protect against rotenone-induced apoptosis (10) and 6-OH-dop-induced cytotoxicity (11) by preserving mitochondrial function (12). Recently, a mitochondrial-targeted H_2S donor, [10-oxo-10-[4-(3-

thioxo-3H-1,2-dithiol-5-yl)phenoxy]decyl]triphenyl-phosphonium (AP39), was synthesised (13, 14). AP39 has shown potential in improving the mitochondrial bioenergetics in SHSY-5Y cells, a thrice cloned subline of the neuroblastoma cell line SK-N-SH, and reduced H_2O_2-induced mitochondrial impairments by abrogating the generation of mitochondrial ROS (8). Moreover, in a rat model of neurological ischemia induced by 90-min middle cerebral artery occlusion, AP39 has been shown to modulate neuroinflammation *in vivo* by reducing cytokine release in brain areas affected by ischaemia (15).

Presently, animal studies with AP39 have required multiple injections for drug administration, either intravenous or intraperitoneally over the course of up to several months (15, 16). Such approaches are difficult to translate to the clinic owing to their painful nature as well as requiring costly professional administration. Transdermal drug delivery systems offer a patient-friendly alternative solution with the additional benefit of offering sustained drug delivery (17). The skin is however a multi-layered organ with the uppermost layer, the stratum corneum, posing an effective barrier to exogenous substances owing to the corneocyte cells embedded in a lipid matrix. To overcome the stratum corneum, chemical permeation enhancers such as propylene glycol, oleic acid or surfactants which reversibly decrease skin barrier function by disrupting intercellular stratum corneum lipids are often employed (18). The drug may then permeate across the skin and into the bloodstream where it can distribute as it would following an intravenous injection (19, 20). Furthermore, drug permeation profiles can be modulated by the choice or amount of permeation enhancer.

The clinical use of H_2S-donors requires the development of safe and effective formulation systems to give a controlled release of H_2S. In this study, we sought to investigate the feasibility of transdermal delivery of AP39 in an aqueous gel using a penetration enhancer, propylene glycol (PG) and explored the ability of permeated AP39 to retain biological functions in scenarios of mitochondrial dysfunction induced by 6-OH-dop, a well-established approach to mimic PD *in vitro*.

2. Materials and methods

2.1 Materials

Hydroxypropyl methylcellulose (HPMC) (catalogue #09963, CAS #9004-65-3) and polyethylene glycol (grade ≥ 99.5%, catalogue #W294004, CAS #57-55-6) was obtained from Sigma-Aldrich (Dorset, England). AP39 was obtained from Cayman Chemical (catalogue #17100, CAS #1429173-57-8) (Michigan, USA). All other reagents including trifluoroacetic

acid, ethanol and acetonitrile were obtained from Fisher Scientific. Ultrapure water was obtained from a Milli-Q purification system (Millipore, Billerica, Massachusetts, US).

2.2 Cell Culture and Treatment

Human neuroblastoma SHSY-5Y cells were maintained in RPMI 1640 (Gibco, Montana, USA) containing 5% FBS and 2 mM glutamine at 37°C in a humidified atmosphere of 5% CO_2. Cells were maintained up to passage 34. SHSY-5Y possess similar characteristics resembling substantia nigra neurons and therefore are routinely used for *in vitro* neurodegenerative research (21).

2.3 Murine Skin Tissue

All animal experiments were performed using procedures permitted by the Aston University Ethical Review Committee in compliance with the UK Home Office Licence Number 3003453 in accordance with the 'Guidance on the operation of animals' under the United Kingdom Animals (Scientific Procedures) Act 1986.

Skin excises were acquired from sacrificed female mice (20–25 g). An animal hair clipper was used to remove the hair from the dorsal portion. Following, the full-thickness skin was harvested and the fat adhering to the dermal side was removed with a scalpel and isopropyl alcohol (>98%).

2.4 AP39 Loaded Aqueous Gel Formulation

HPMC aqueous gels were prepared at 5% w/v in distilled and deionised water and mixed overnight using a mechanical mixer (Polytron PT 3100 D) at a speed of 3000 rpm. Gels with an AP39 loading of 0.002% w/v were manufactured with either 0 or 10% v/v PG by adding the required amount of AP39, dissolved in ethanol, to the prepared gels and mixing for 1 h. Both gel preparations contained 5% v/v ethanol.

2.5 HPLC Methodology and Validation

Detection of AP39 was assessed using a reverse phase HPLC methodology. A Shimadzu LC-2030C Plus RoHS - Prominence-I separation module HPLC with UV detection was utilised at an operating wavelength of 242 nm. A Phenomenex HyperClone™ column (5µm C18 4.6 x 150 mm column) was used with a 2.5 µL sample injected at 27°C. Samples were kept at 4°C while inside the Autosampler. An isocratic method was developed with the mobile phase comprising of a 87.5:12.5 ratio of 0.01% TFA in acetonitrile to 0.01% TFA in ultrapure water at a flow rate of 1.25 mL/min. Stock solutions and standard solutions of AP39 were prepared in ethanol ranging from 0.0001-1 mg/mL. Numerous chromatographic conditions were systematically tested including; the mobile phase composition (solvent ratio and composition)

flow rate, injection volume, and autosampler temperature, to optimise the method before validation. A final calibration curve with an R^2 of 0.998 and a linear equation of y = 5177240 · x – 3055 was obtained.

The method was validated by assessing the linearity and range, repeatability (precision) and sensitivity in terms of the limit of detection (LOD) limit of quantification (LOQ) and precision. The system was flushed with 50% acetonitrile and water before each use for 45 min. For the linearity and range assessment, standard solutions ranging between 0.0001-1 mg/mL of AP39 in ethanol were prepared. The mean peak area ± SD was calculated and then plotted against known concentrations of the standard. The repeatability of the developed method was assessed by determining the interday (over three days) variability. The sensitivity of the method was assessed by calculating the LOD (equation 3.2), and the LOQ (equation 3) from the standard deviation (Equation 1). Calibration curves carried out during the linearity assessment were used to determine the standard deviation of the response (σ) and the slope (S) . Finally, as per the ICH guidelines (Guideline, 2005), a signal-to-noise ratio of three was assumed for the LOD quantification, whereas for the LOQ, a signal-to-noise ratio of ten was applied.

Equation 1: Standard deviation $\sigma = \sum(y - y_i)^2 / n^2$

Equation 2: Detection limit $LOD = 3.3 \times \sigma / s$

Equation 3: Quantitation limit $LOQ = (10 \times \sigma) / s$

where σ is the standard deviation of the response based on the residual standard deviation of the regression line, y is a data value, y_i is the mean, n is the total sample population, and finally, s is the slope of the calibration curve.

2.6 Determination of AP39 Solubility and Stability in gel formulations

1 part gel was mixed with 9 parts of ethanol for HPLC-UV detection and quantification. Gels were stored at room temperature and samples were taken weekly over a four-week period for analysis.

2.7 Texture Analysis of Gel Formulations

The adhesive capacity of both formulations was measured using (Stable Micro System Texture Analyser TA. XT. Plus). The adhesive test settings were set as follows; test speed = 0.5 mm/sec, contact time = 5 s, force applied = 100 g, trigger force = 5 g. The maximum force (N) was recorded from the texture analysis graph, and the results were presented as mean ± SD of five points.

2.8 Viscosity Analysis of Gel Formulations

Formulation viscosity: The viscosity of the formulations was calculated using a micro viscometer Microvosc (RheoSence, USA), through injecting 100 µl of sample at 32 °C with a shear rate of 50 s^{-1}.

2.9 Gel Release Study on Excised Murine Skin

Permeation studies were carried out *in vitro* with Franz diffusion cells (PermeGear, Hellertown, PA, USA) for the assessment of PG's ability to improve the flux of AP39 across skin. The system was maintained at 35°C using a shaking incubator set at 20 RPM to prevent any diffusion layer effects during the study (LSE, 49 L, Corning). The cell's orifice diameter was 11.28 mm, the effective diffusion area was 1.00 cm^2 and the receptor volume was 8 mL. Murine skin (epidermis layer of average thickness 0.34 ± 0.02 mm) samples were cut, washed, and used immediately following excision. Skin samples were carefully mounted on the receptor chamber of a vertical Franz Diffusion cell. The receiver compartment was carefully filled with PBS:ethanol (90:10) to ensure no air bubbles next to the skin. After the assembled Franz cell was equilibrated for at least 30 min, 0.2 mL of each gel formulation was applied to the skin. Over the course of the study, the diffusion systems were shaken at 20 RPM to prevent any diffusion layer effects. At 1, 2, 4, 6, 8 and 24 h, 200 µl of the receptor medium was withdrawn, and the same volume of fresh buffer solution was replaced to the receptor chamber. The concentration of the samples was assayed with HPLC-UV as described in section 2.5.

The *In vitro* drug release kinetics were assessed as described previously using Microsoft Excel®. Zero order, first order and Higuchi release profiles were applied to release from each formulation following which regression analysis techniques were employed to determine the probable drug-release (22). The release kinetic model displaying the highest r^2 metric (≥ 0.95) was determined to be the mechanism, by which release occurred.

Furthermore, the lag time for gel formulations was calculated from the release study by extrapolating the tangent of the curve from the first 4 h (steady state) to the X-axis; this line intersects with the time axis at some point where the amount of drug is zero; this time is called lag time (t_{lag}).

2.10 Microvasculature Endothelial Cell Model

Primary Human Umbilical Vein Endothelial cells (HUVEC, PromoCell, Cat. # C-12203) were cultured in full growth media (EGM-2) (PromoCell, Cat. # C-22211) supplemented with Fetal Calf Serum 0.02mg/mL, Epidermal Growth Factor 5ng/ml, Basic Fibroblast Growth Factor 10 ng/ml, Insulin-like Growth Factor 20 ng/mL, Vascular Endothelial Growth Factor 0.5ng/mL,

Ascorbic Acid 1µg/mL, Heparin 22.5 µg/mL, Hydrocortisone 0.2 µg/mL (supplement kit, Promocell, Cat. # C-39211) and 5 mL of 1X Penicillin/Streptomycin (Lonza, Cat. # LZDE17-602E) (Promocell, Heidelberg, Germany). Culture medium was changed every 48 hours and cells were incubated at 37°C in a 5% CO_2 humidified atmosphere incubator. Cells were sub-cultured at 70-80% confluency and up to passage 5. Before each treatment cells were starved using 5% FBS (Gibco, Cat. # 11550356) M199 starvation media (Lonza, Cat. # LZBE12-119F) supplemented with antibiotics for 2 hours (Lonza, Basel, Switzerland). To ensure the quiescent state of the cells and consistent results, treatments were diluted in the starvation media unless otherwise stated.

HUVEC cells were seeded (3×10^5/ml) onto 24-well polycarbonate inserts (23) and cultured for 4 days. On the fifth-day tight-junction formation was enhanced through the addition of 250 µM cAMP, 17.5 µM RO 20–1724 and 550 nM hydrocortisone in the absence of serum for 24 h prior to the initiation of an assay (24) (Figure 1). Barrier integrity and formation was assessed through the determination of the transendothelial electrical resistance (TEER), which was measured on day 3 and day 4 using a chop-stick electrode (World Precision Instruments STX2).

2.11 Drug Transport Assay

HUVEC cells were grown on permeable inserts as described in section 2.10 and placed into a 24-well cell culture plate. Release media collected following the murine skin permeation study (section 2.9) was diluted 1:4 with serum-free culture medium and added to the apical compartment with sampling taking place from the opposite compartment, and replaced with equal amounts of serum-free culture medium (Figure 1).

AP39 concentrations were analysed using the HPLC method described in section 2.5.

The apparent permeability (P_{app}) was calculated using the equation below,

$P_{app} = (dQ/dt) / C_0 \times A$

where dQ/dt is the amount of drug permeated per unit time, calculated from the regression line of time points of sampling, C_0 the initial drug concentration in the donor compartment and A (cm^2) is the insert surface area (0.33 cm^2).

2.12 H_2S Release from Permeated AP39

Free H_2S reduces tetrazolium dye 3-(4,5-dimethyl-2-thiazolyl)-2,5-diphenyl-2H-tetrazolium bromide (MTT, Sigma, St. Louis, MO) and therefore forms the purple/indigo colour, formazan (14). Thus, to evaluate H_2S release, from the AP39 in the drug transport assay (section 2.11), 100 µL of cell culture media was removed from the basal section of the transwell at 30, 60 and

90min and added to 100 µL MTT (5 mg/mL) for 3 h. As described previously, this reaction was carried out in a humidified incubator at 37 °C with 5% CO_2 atmosphere. Changes in UV absorbance were observed on a plate reader at 570 nm. A H_2S calibration curve was created by preparing serial dilutions of freshly dissolved sodium sulphide (Na_2S). The H_2S generation is shown as a change in absorbance over 90 min with respective H_2S concentration values.

2.13 Detection of Mitochondrial Reactive Oxygen Species (mt-ROS)

The generation of mt-ROS was detected using the fluorescent probe MitoSOX Red (Sigma Aldrich, Dorset, England) by fluorescent microscopy as previously reported (8). Briefly, cells were plated on coverslips (2.0×10^5 cells/coverslip) and exposed to permeated AP39 or 6-OH-dop (10 µM) alone or in combination for 24 h in the incubation conditions previously described. Afterwards, coverslips were washed in warm PBS and incubated with MitoSOX Red (5 µM) in PBS for 30 min, at 37°C and protected from light. Coverslips were then gently washed with PBS and fixed with 4% paraformaldehyde for 30 min. Lastly, coverslips were mounted in glass slides using the SlowFade™ Diamond Antifade Mountant (Invitrogen, Massachusetts, USA). Fluorescence emitted at 580 nm was recorded and analysed using a Nikon Eclipse Ti-E inverted microscope with a 60× objective.

2.14 Cellular Bioenergetics

Parameters of the mitochondrial function were assessed using an XFe24 Extracellular Flux Analyser (Agilent Technologies, Santa Clara, USA) following protocols established in our lab (8, 25). Briefly, SHSY-5Y were plated at 5.0×10^4 cells/well using V7 24 well plates (Agilent Technologies, Santa Clara, USA) and cells left to attach overnight at 37°C in a humidified atmosphere of 5% CO_2. Following this, cells were washed and media replaced with non-buffered DMEM (10 mM glucose, 1 mM pyruvate and 2 mM L-glutamine) to allow temperature and pH equilibrium. Permeated AP39 and/or 6-OH-dop (10 µM) was added for 24 h. Oxygen consumption rates (OCR) were measured initially to calculate basal respiration rates. Following, the sequential injections of oligomycin (1 µM) (Sigma Aldrich, Dorset, England), carbonyl cyanide 4-(trifluoromethoxy) phenylhydrazone (FCCP) (0.5 µM) (Sigma Aldrich, Dorset, England) and a mixture of rotenone and antimycin A (Rot/AA) (1 µM) (Sigma Aldrich, Dorset, England), (75 µL per injection) allowed to inhibit the ATP synthase, uncouple oxidative phosphorylation, and inhibit complex I and complex III-dependent respiration. The sequential administration of these compounds allowed to calculate, parameters of the mitochondrial function, including basal, maximal respiration, spare respiratory capacity, ATP- linked OCR and proton leak to be determined. Data were expressed as the rate of oxygen consumption ($pmolO_2$/min/µg protein) by time. The concentration of proteins per well was assessed using BCA protein assay (Bio-Rad) after the completion of Seahorse assays.

2.15 Statistical Analysis

All results are presented as mean ± standard deviation (SD). Two replicates of at least three independent studies were used unless otherwise stated. For multi-well plate cells assays, replicates of six were used for each experimental condition, repeated three times. When two groups were compared, a t-test was used, whereas any statistically significant difference between means of three or more groups was assessed with one-way ANOVA with a post-hoc Tukey's multiple comparisons test applied to evaluate differences between groups. A p value ≤ 0.05 was considered statistically significant. All calculations were completed on GraphPad 8.1.0 (GraphPad Inc., La Jolla, California, USA).

3. Results

3.1 HPLC Methodology and Validation

Stock solutions and standard solutions of AP39 were prepared in water ranging from 0-1 mg/mL. Calibration data using the method outlined in section 2.5 was then obtained (Supplementary figure 1 and 2).

To assess the linearity and range of the HPLC-UV method developed for the separation and detection of AP39, concentrations ranging from 0.0001-1 mg/mL in ethanol were prepared. The method established demonstrated a high correlation with a good linear fit, with a correlation coefficient (R^2) greater than 0.99 (Supplementary figure 2A). Assessment of repeatability/precision of the method was assessing by observing the interday (over three days) variability (Supplementary figure 2B). Results showed that AP39 standards from 0.0001-1 mg/mL have no statistically significant difference for all the calibration curves carried out on different days, demonstrating the method has reliable precision.

Study of the sensitivity of this method was assessed by calculating the limit of detection (LOD) and the limit of quantification (LOQ). Values from the calibration curve determined from the linearity assessment were used to determine the standard deviation of the response (σ) and the slope (S). Therefore, following Equations 2 and 3, the sensitivity of the method for AP39 was calculated; the LOD and LOQ was 0.0151 mg/mL and 0.0457 mg/mL respectively.

3.2 Determination of AP39 Solubility and Stability in Gel Formulations

The stability of the AP39 in both gel formulations was assessed by measuring drug concentration over 28 days with HPLC-UV detection (Figure 2). AP39 solubility was maintained only in the formulation with PG, the gel formulated with no PG showcased a decrease in AP39 concentration over this time period ($p<0.01$). Upon visual inspection, the

precipitated drug was observed at the bottom of the vial suggesting the drug did not remain soluble in the formulation without PG over the 28 days.

3.3 Rheological Behaviour of the Formulated Gels

To determine the rheological properties of gels prepared with or without PG we investigated parameters describing the gel adhesiveness, and viscosity (26) (Table 1). Such properties must be defined not only to assess gel adhesiveness to the skin but to ensure formulation reproducibility. The adhesiveness of the designed transdermal delivery systems was investigated and reported as the average maximum force. The presence of PG caused a reduction in the adhesive force from 488.05 ± 12.41 to 432.44 ± 6.77 N ($p<0.05$) suggesting this formulation would adhere to the skin less. Furthermore, the viscosity of the gels was assessed at 32°C, the average temperature of the skin. The addition of PG to the formulation significantly decreased the viscosity from 682.88 ± 5.99 to 648.53 ± 5.08 mPA*s ($p<0.05$) suggesting this formulation may be easier to spread across the skin.

Table 1: Texture Analysis of Gels to Show Adhesive Capacity and Viscosity at 32 °C.

Formulation	**Adhesive force (N)**	**Viscosity (mPA·s)**
0% PG	488.05 ± 12.41	682.88 ± 5.99
10% PG	432.44 ± 6.77	648.53 ± 5.08

3.4 Effect of propylene glycol on the Flux of AP39 Though Excised Murine Skin

The permeation of AP39 through *ex vivo* murine skin samples was assessed for the two gel formulations. PG was observed to increase the permeation of AP39 across the murine skin approximately by 2-fold. We observed that in formulations containing 0% v/v PG, 24.40 ± 2.39 % of applied AP39, permeated across the skin compared with 48.59 ± 2.93 % from gels formulated with 10% v/v PG. Thus, a significant difference in permeated AP39 was observed across 24 h between the two formulations ($p<0.0001$) (Figure 3). Finally, the t_{lag} decreased significantly from 1.82 (±0.02) to 0.86 (±0.01) in the presence of 10% v/v PG ($p<0.0001$).

The determination coefficient (R^2) and Akaike Information Criterion (AIC), suggested the model that fit AP39 release from the gel formulation with 0% v/v PG was the first order model (K_1 0.013 ± 0.001) and for the gel with 10% v/v PG it was the Higuchi model (K_H 9.40 ± 0.48) (highest R^2 and lowest AIC) (Table 2).

Table 2: *Ex vivo* AP39 Release Kinetics Models.

		HPMC gel formulated with PG	
Kinetic model	Parameter	0 % v/v	10 % v/v
0	k_0 (mg.min^{-1})	1.129 ± 0.077	2.29 ± 0.119
	R^2	0.784 ± 0.073	0.713 ± 0.048
	AIC	23.348 ± 1.702	29.904 ± 0.931
1st	k_1 (min^{-1})	0.013 ± 0.001	0.033 ± 0.002
	R^2	**0.836 ± 0.060**	0.888 ± 0.030
	AIC	22.292 ± 2.014	25.030 ± 1.445
Higuchi	k_H	4.451 ± 0.219	9.404 ± 0.480
	R^2	0.773 ± 0.054	**0.940 ± 0.015**
	AIC	24.100 ± 2.382	22.001 ± 1.288

R^2, coefficient of determination; AIC, Akaike Information Criterion; F is the fraction of AP39 released at time t; k_0 is the zero-order release constant; k_1 is the first-order release constant; k_H is the Higuchi release constant. Bold text signifies the highest R^2 value. Results are presented as mean ± standard deviation (n=3).

3.5 Trans-endothelial Electrical Resistance (TEER) of HUVEC Microvasculature Model and Apparent Permeability Determination

To investigate the formation of a high resistance barrier, the TEER values from monolayers of HUVECs' grown on permeable inserts (24-well, 0.33 cm^2) were determined. Endothelial tight junction-inducing agents were added to cells for 24 hours. On day 5 post seeding, TEER values were determined. On day 5, TEER values significantly increased from 74.46 ± 5.11 Ω.cm^2 to 149.05 ± 9.18 Ω.cm^2 ($p < 0.0001$) (Supplementary Figure 3). The permeability of AP39 transported across the skin from gels formulated with 10% v/v PG across HUVECs that were grown on permeable inserts was assessed. The total cumulative amount of AP39 transported/permeated was 6.16 ± 0.19 mcg/ mL over 90 min. The apparent membrane permeability (P_{app}) was 18.06 ± 1.42 x 10^{-6} cm/s (Figure 3A).

3.6 H_2S Release from permeated AP39

To ensure permeated AP39 maintained the capability to release H_2S, conditioned media with AP39 following the apparent permeability studies from gels formulated with 10% v/v PG, was investigated for levels of H_2S over 90 min. Maximum H_2S release was detected within 30 min (Figure 4B) and levels of H_2S decreased quickly. By 90 min, H_2S levels were reduced to a minimum level (Figure 4B). This suggests that from the moment AP39 is in the cellular environment, it releases H_2S rapidly and is reduced to a minimum over the course of 180 min in total (including the time of the permeation study prior to this H_2S release assay).

3.7 Permeated AP39 Protects the Mitochondrial Function in 6-OH-dop Exposed SHSY-5Y

Once we determined that permeated AP39 retained the ability to release H_2S, we evaluated the potential of permeated AP39 to sustain biological effects in scenarios mimicking Parkinson's Disease (PD) *in vitro*. To resemble the condition of PD, 6-hydroxydopamine (6-OH-dop) has been administered to rats by intracerebral infusion, leading to the destruction of dopaminergic neurons and behavioural dysfunction (27). Moreover, 6-OH-dop has been employed *in vitro* to emulate the condition in cells to investigate the molecular and biochemical mechanisms underlying neurodegeneration (28). To evaluate the potential of permeated AP39 to abrogate 6-OH-dop-induced mitochondrial dysfunction without affecting cellular viability, we explored different concentrations of 6-OH-dop ranging from 10-100 μM (IC50 = 100 ± 9) (29) and assessed their effects on SHSY-5Y viability (Supplementary Figure 4). At 10 μM 6-OH-dop did not affect the viability of SHSY-5Y whereas a concentration of 6-OH-dop ranging from 50-100 μM reduced the cells viability by 75% ($p<0.0001$) (Supplementary Figure 4). For further experiments, we employed 10 μM of 6-OH-dop to establish a model of "mitochondrial dysfunction" mimicking PD in SHSY-5Y.

We assessed the cellular bioenergetics on SHSY-5Y exposed to 6-OH-dop, permeated AP39 or both in combination. We explored in real-time, traces of oxygen consumption rates (OCR) after the sequential administration of mitochondrial modulators: oligomycin, FCCP and a mixture of rotenone and antimycin A. We observed that 6-OH-dop significantly reduced the OCR values (Figure 5A), which resulted in reduced mitochondrial efficiency as observed by a dramatic reduction in basal respiration ($p<0.005$) and maximal respiration ($p<0.005$) parameters, in comparison to control cells (Figure 5B). Moreover, permeated AP39 did not affect mitochondrial respiration parameters when compared to control cells. Interestingly, we observed that the combination of permeated AP39 and 6-Oh-dop resulted in enhanced OCR values when compared to 6-OH-dop alone. In this regard, the administration of permeated AP39 to 6-OH-dop treated cells resulted in significant improvement of the basal respiration ($p<0.05$), maximal respiration ($p<0.05$) and ATP-linked OCR ($p<0.05$) when compared to cells exposed to 6-OH-dop only. There was no difference between OCR levels measured in control

cells when compared to those exposed to PD inducer 6-OH-dop in combination with permeated AP39 (Figure 5B).

Once we observed that permeated AP39 retained mitochondrial targeted effects, we tested whether permeated AP39 would retain antioxidant effects in PD-like environment. We observed that 6-OH-dop induced the generation of mitochondrial-specific reactive oxygen species (mito-ROS), measured by fluorescence microscopy using the fluorescent probe MitoSOX Red. When administered in combination to 6-OH-dop, permeated AP39 abrogated mito-ROS observed as a qualitative reduction in red fluorescence when compared to cells only exposed to 6-OH-dop (Figure 5C). These results suggest that AP39 permeated through the skin in formulated gels, retain mitochondrial targeting properties and has effects on mitochondrial function, we suggest these novel formulation approaches for AP39 may be suitable to explore in neurodegenerative conditions such as PD.

4. Discussion

Hydrogen sulphide (H_2S) has been recognised to have a crucial role in many physiological and pathophysiological processes and has recently been proven to have protective roles within the brain (5) emphasising its therapeutic potential in the treatment of neurologic conditions. In this regard, AP39, a mitochondrial targeting H_2S donor may hold promise in conditions associated with dysregulated mitochondrial function, such as PD. However, a key challenge concerns the delivery of H_2S donors at a sustained rate, to allow maximum H_2S bioavailability with minimal possible toxic effect. To overcome these constraints, in this study, we developed a transdermal delivery system for AP39. We provided evidence that AP39 can gradually flux across *ex-vivo* murine skin and that the permeated AP39 is able to sustain the release of H_2S, whilst maintaining its biological effects on the mitochondria. To the best of our knowledge, this is the first report showing the feasibility of formulating AP39 for transdermal application, we suggest that this delivery system of AP39 has the potential to avoid repeated dosing as well as injections and offer a patient-friendly alternative to alleviate mitochondrial dysfunction in detrimental neurological scenarios.

Propylene glycol is popular in the formulation of transdermal preparations owing to its ability to increase dermal permeation by altering lipid packing (30). The mechanism of action of PG in enhancing drug permeation is not clearly understood, however, it may be attributed to a possible “carrier-solvent“ effect (31), dehydration (32, 33) or an increased solubility in intercellular lipids of the stratum corneum (34). PG increased the permeability of AP39 across excised murine skin. Gels formulated without PG observed less cumulative transport across the skin with more AP39 remaining in the gel and the skin. Moreover, PG improves the solubility of low-water soluble drugs, a property particularly desirable for low-solubility drugs

such as AP39 (35). Indeed, we observed that HPMC carrier formulated with PG increased the solubility and stability of AP39 within the aqueous gel formulation. However, PG is known to modify the characteristics of hydrogen bonding between water, solvent, and polymer, affecting the bioadhesive properties of the gel (36, 37). Adhesiveness and viscosity are such properties correlated to gel bioadhesiveness, a parameter of great importance in transdermal preparations. Adhesion is the intermolecular attractive force between molecules of a different kind or phase, in this case, adhesion between the gel and the skin. Gel's adhesiveness affects how the gel interacts with the skin thus allowing absorption, weak adhesion translates to weak absorption and lower dose (38). We observed that the incorporation of PG in the aqueous gel caused a decrease in adhesive forces as well as viscosity. Similar to our study, an investigation into the effect of PG on chitosan gel also observed PG caused a decrease in adhesive properties (39). Furthermore, PG has previously been observed to decrease the surface tension and viscosity of emulsions and HPMC transdermal preparations (40, 41). Whilst the observed decrease in adhesiveness of formulations with PG may reduce the dose absorbed, the reduction in viscosity would make it easier to spread a thin layer across the skin to mitigate for this. Further studies to observe this effect on skin are required to optimise PG loading for optimal dermal permeation.

The presence of PG within the formulation increased the rate of transdermal flux AP39. The release of AP39 from the formulation with no PG was in favour of the first-order model demonstrating drug release was in proportion to the amount of drug available at that time. This was in contrast to the formulation with PG where the release was in favour of the Higuchi diffusion model indicating a diffusion-controlled mechanism of AP39 release in which the amount of drug released was proportional to the square root of time and the rate of release is proportional to the square root of drug solubility, exposed surface area, diffusion constant and inverse time (42). Previous studies within our group assessing the dermal permeability of ADT-OH, a non-targeted H_2S donor, observed similar results with PG increasing transdermal flux in a concentration-dependent manner (17). PG has been reported to enhance percutaneous drug absorption by solubilising α-keratin within the dermal corneocytes (43). Furthermore, a decrease in viscosity may also be reflected with an increase in drug diffusion and therefore dermal permeation (40, 44).

The development of drug treatments for brain delivery is particularly challenging due to the presence of the blood-brain barrier (BBB). The BBB separates the systemic circulation from the cerebral parenchyma and is composed of cerebral capillary endothelial cells connected by tight junctions which contribute towards reduced permeation of small-molecule drug permeability (45). Our study observed that formulated AP39 was able to permeate across a cellular barrier model and release H_2S. Previous studies *in vivo* have observed that when

AP39 in solution was delivered to mice, an increase in H_2S levels in the brain cortex was observed (46). Moreover, it has been reported that the intraperitoneal administration of AP39 has provided protection against renal ischemia (15). This evidence shows that AP39 is a suitable candidate to address mitochondrial dysfunction in PD, however, the extensive dosage regimes that would have to be imposed in order to achieve these effects (from six to twelve weeks, daily intraperitoneal injections), suggest their translation to the clinic would encounter many difficulties due to their lack of patient-friendly approach. Our study not only showed that AP39 can successfully be formulated in gels and permeate through murine skin, we also observed that a maximum H_2S release was observed within 30 min of AP39 crossing a microvasculature barrier; this suggested the controlled release potential of the transdermal delivery system for AP39 will assist in providing sustained delivery of AP39 thus H_2S release within the target organ, providing a more patient-suitable approach with potential to translate to the clinic. Our observations also explored the potential of permeated AP39 to exert mitochondrial effects. In this regard, there are different mechanisms by which H_2S exerts neuroprotective effects in scenarios resembling PD, including anti-oxidant, anti-inflammatory, anti-apoptotic, and pro-survival signalling. Particularly, H_2S donors such as AP39, have been found to decrease mitochondrial oxidative stress through its cytoprotective effects and the ability to reduce the mitochondrial DNA oxidative damage (13). Moreover, AP39 possess the potential to reduce cytokine release in rats' brain and modulate neuroinflammation (8). In addition, AP39 protects cultured endothelial brain cells against oxidative stress (47). Our study showed that permeated AP39 abrogated mitochondrial-specific reactive oxygen species in a model of PD in vitro, established with the neurotoxin 6-hydroxydopamine. We also observed that permeated AP39 enhanced ATP generation, increasing parameters of the mitochondrial function. These evidence shows that AP39 formulated into gels can retain its biological properties *in vitro*.

5. Conclusion

The transdermal delivery of AP39 is an encouraging patient-friendly therapeutic option in the treatment of various neurodegenerative disorders such as PD with the potential to offer sustained H_2S levels in the circulation thus reducing toxicity and dose frequency. Aqueous gels prepared with 10% v/v propylene glycol maintained the solubility of AP39 over 28 days and increased AP39 permeation through *ex vivo* murine skin samples. Additionally, permeated AP39 was able to pass through a HUVEC microvasculature model and release H_2S. Permeated AP39 was then observed to reduce mitochondrial-specific reactive oxygen species in a 6-hydroxydopamine model of PD *in vitro*. Finally, permeated AP39 enhanced ATP generation, increasing parameters of the mitochondrial function. Taken together, this evidence

demonstrates AP39 formulated into aqueous gels is able to retain its biological effects *in vitro* and thus is a worthy and viable alternative to injectable delivery methods.

6. Contributions

MKM and LSA conceptualised the study and revised the intellectual concept of the work. MKM, LSA, BM, MI, RS and MAAT performed experiments, analysed the data and participated in the generation of a first draft of the manuscript. MKM, LSA, HS, RS, SA, KW and KR edited the manuscript and revised critically the intellectual nature of the final draft. All authors approved final version for submission. LSA secured funding for this work.

7. Funding

This work was supported by the Royal Society Grant - Round 1 2021 (RGS\R1\221169) and by the Sir Halley Stewart Trust (Ref number 2728). The views expressed within this report are those of the authors and not necessarily those of the Trust, both awarded to LSA.

Figures and figure legends:

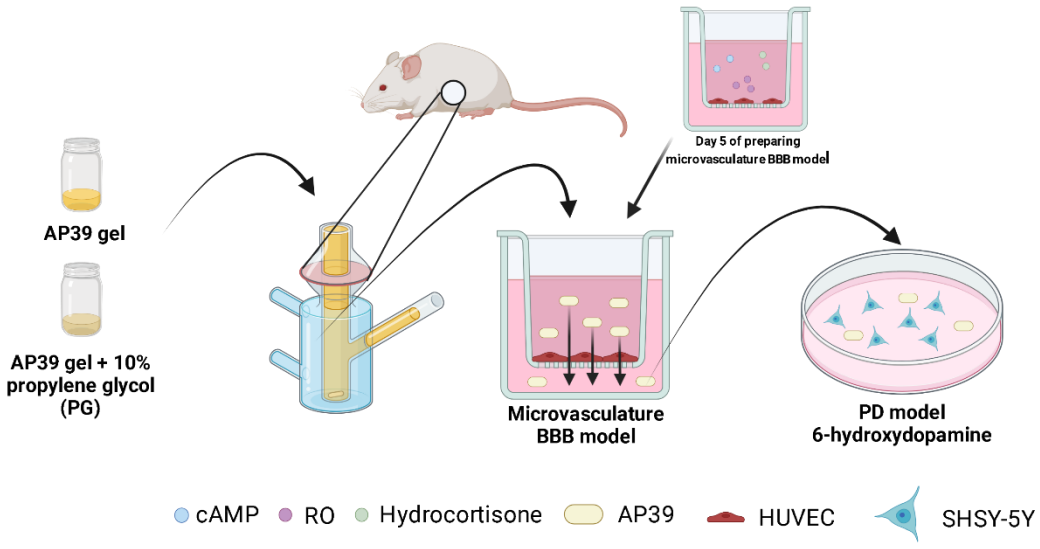

Figure 1. Schematic diagram of experimental set up to assess AP39 flux across ex-vivo murine skin, permeability across BBB model and biological effects on the mitochondria in SHSY-5Y exposed to 6-hydroxidopamine (6-OH-dop). Created with BioRender.com

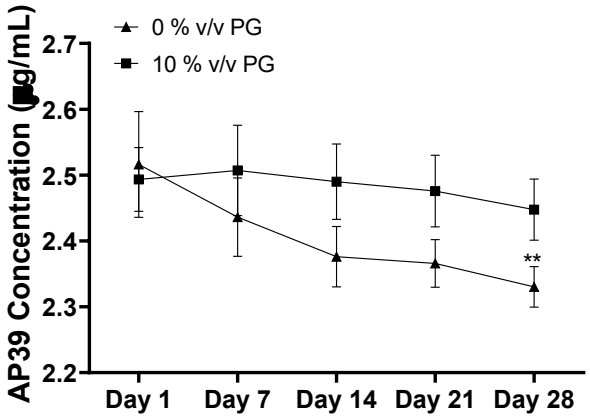

Figure 2. Stability of AP39 in gel formulation over 28 days as determined by HPLC-UV analysis. Results are expressed as mean ± SD and analysed by t-test. n = 3 independent batches. **p < 0.01 vs 0% v/v PG.

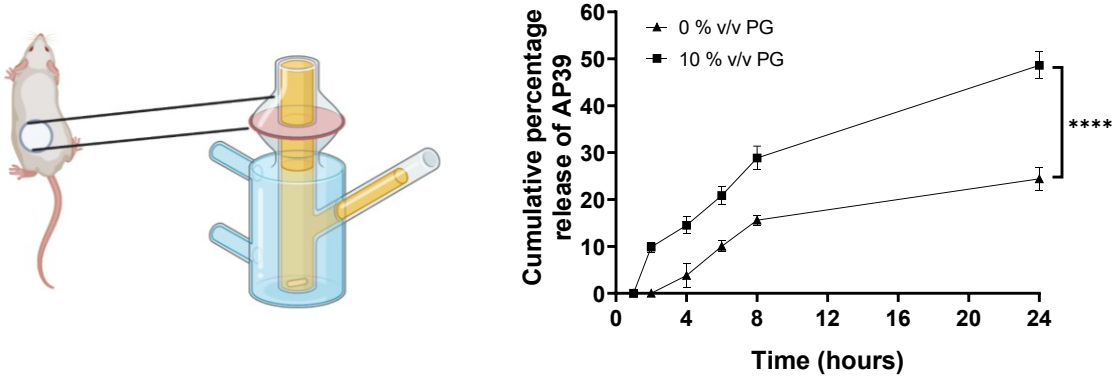

Figure 3. HPMC gels formulated with 10% v/v PG loading in gels loaded with 0.8 % w/w AP39 increased AP39 flux across *ex vivo* murine skin samples compared with 0% v/v PG. Cumulative percentage AP39 release profiles up to 24 h. Release across skin was observed using a Franz cell system and quantified by HPLC-UV analysis. Results are expressed as mean ± standard deviation and analysed by a t-test. n = 3 independent batches. ****p < 0.0001 vs 0% v/v PG.

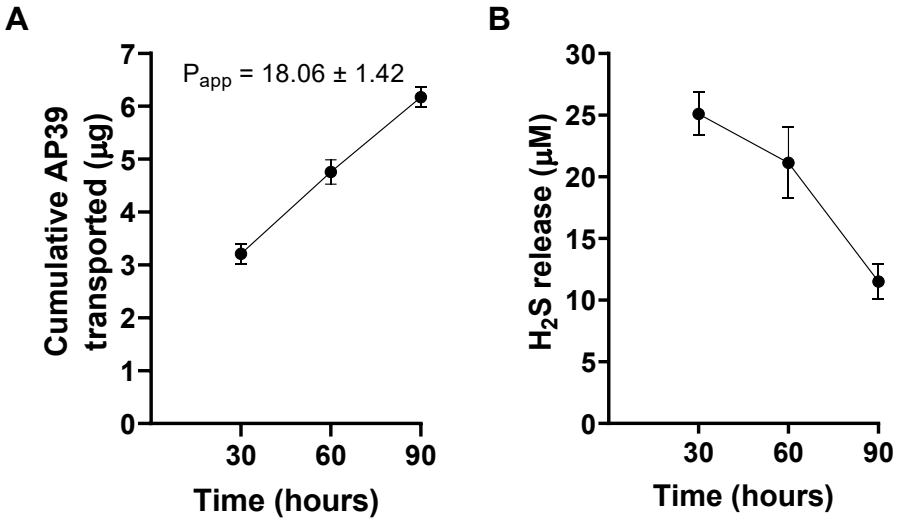

Figure 4. AP39 flux across HUVECs grown on permeable inserts with (A) the apparent permeability coefficient over 90 min, followed by (B) H_2S detection over another 90 min. Results are expressed as mean ± standard deviation. n = 6 in 3 independent experiments.

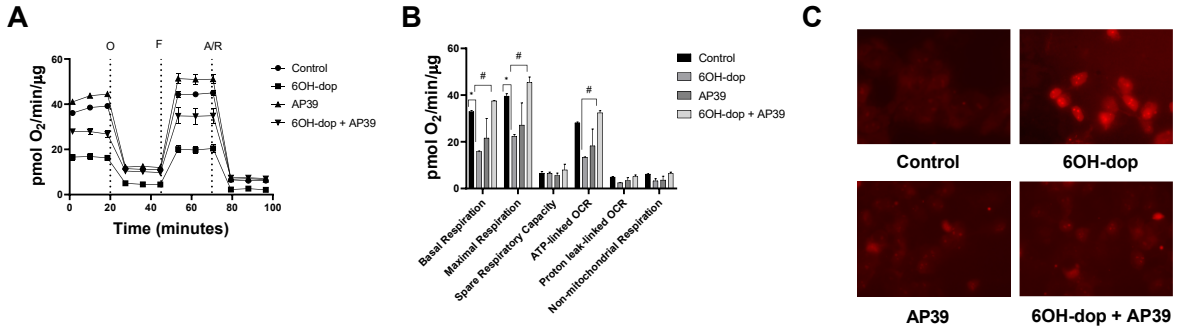

Figure 5. Permeated AP39 retain biological effects on the mitochondria in SHSY-5Y exposed to 6-hydroxidopamine (6-OH-dop). (A) Oxygen consumption rates (OCR) expressed by time were measured using an XFe24 Seahorse Analyser after the sequential administration of mitochondrial modulators; oligomycin (O), carbonyl cyanide 4-(trifluoromethoxy) phenylhydrazone (FCCP) and a mixture of rotenone and antimycin A (A/R). (B) Calculated parameters of the mitochondrial function from data observed in A. n=5 (C) Mitochondrial-specific ROS (mito-ROS) was assessed by fluorescence microscopy using the fluorescent probe MitoSOX Red. Results are expressed as mean ± standard deviation. n=3 independent batches. *p < 0.05 vs control, #p < 0.05 vs 6-OH-dop.

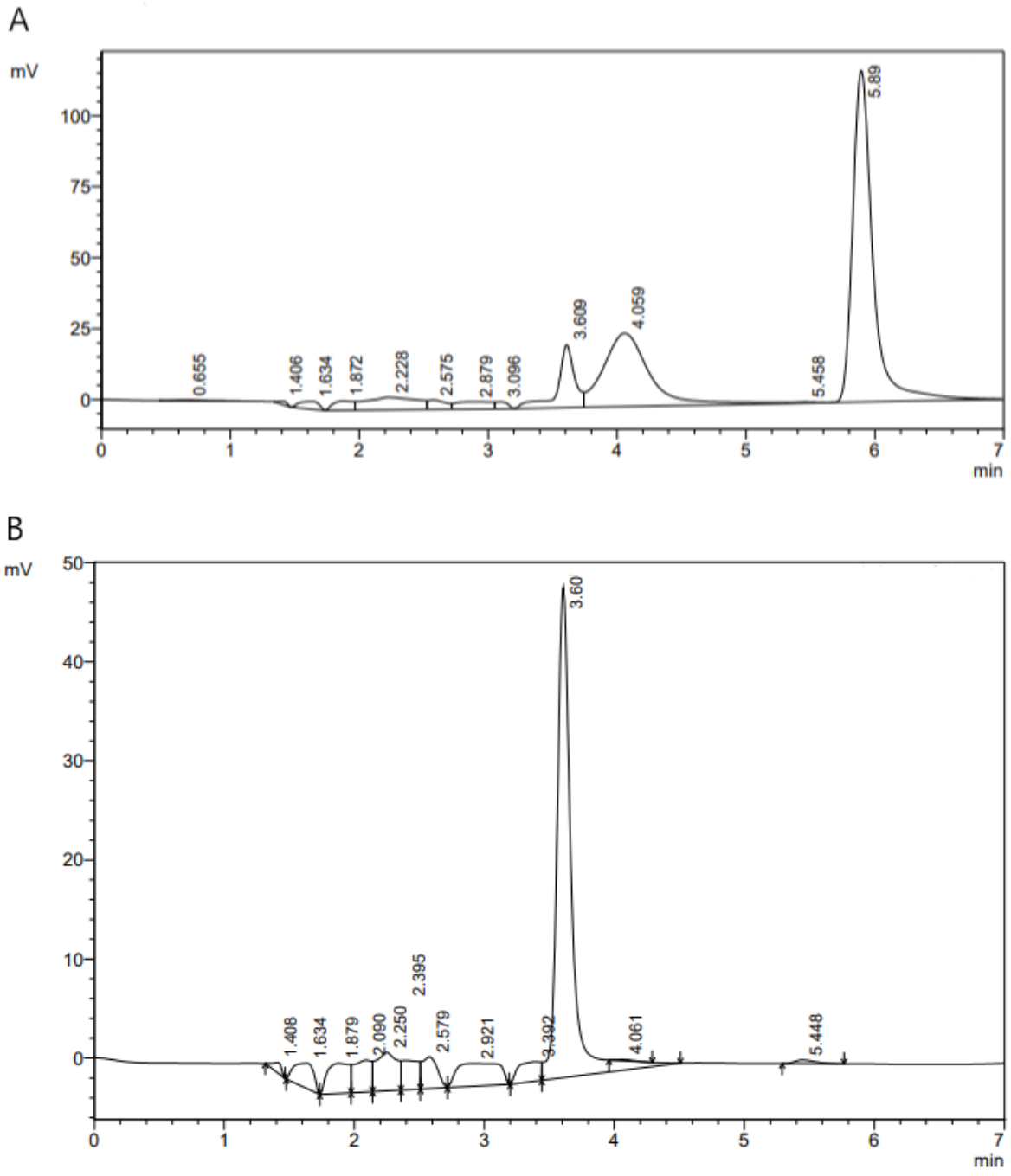

Supplementary figure 1: Typical chromatogram of a) 1 mg/mL and b) 0mg/mL AP39 in PBS:ethanol 90:10.

The retention time of AP39 was observed at 5.89 min. No peak was visible at this time point in blank solutions. The solvent front was observed around 4 min.

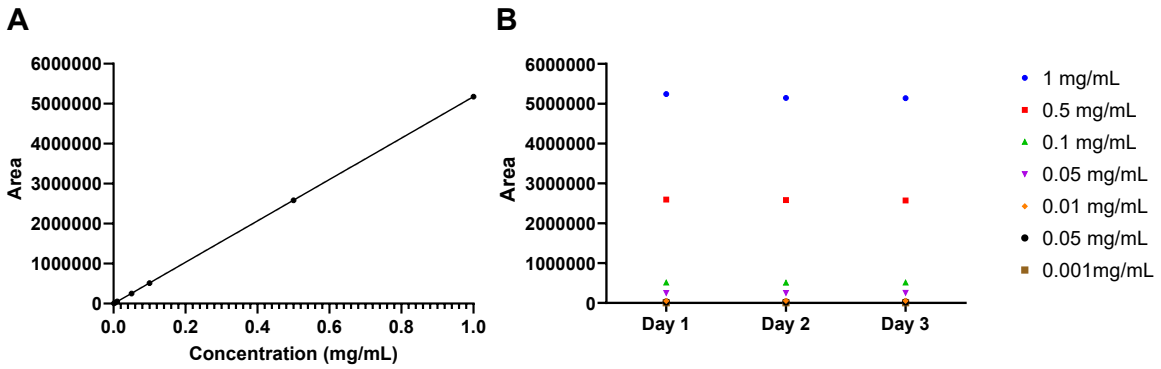

Supplementary figure 2: Calibration data for AP39 as determined by HPLC-UV analysis shows good linearity and reproducibility over 3 days.

Calibration data for AP39 over the concentration range of 0.0001-1 mg/mL in ethanol. a) A proportional response was evident versus the analytical concentration over the working concentration range with an r2 of 0.998 and linear equation of y = 5177240 ·x – 3055. b) reproducibility of AP39 determination over the specified concentration range was constant over 3 different days. Data represents mean ± SD. n=9 in 3 independent batches.

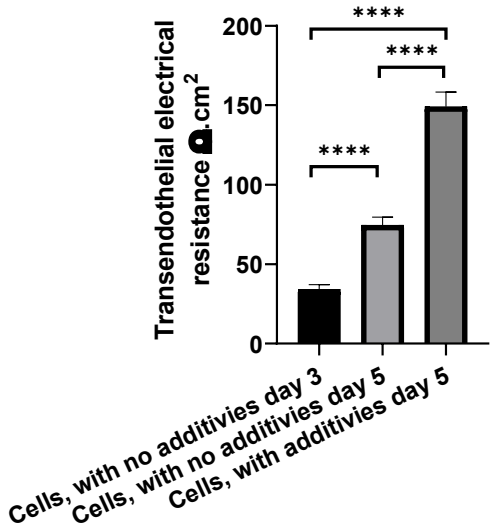

Supplementary figure 3. TEER values were measured following growth of HUVEC cells on permeable cell culture inserts (24-well, 0.33 cm2) under static conditions. TEER of HUVEC were measured when grown on permeable inserts in the (A) absence and (B) presence of barrier-forming additives. ****p ≤ 0.0001. n = 9 in in 3 independent batches and analysed by an one way ANOVA .

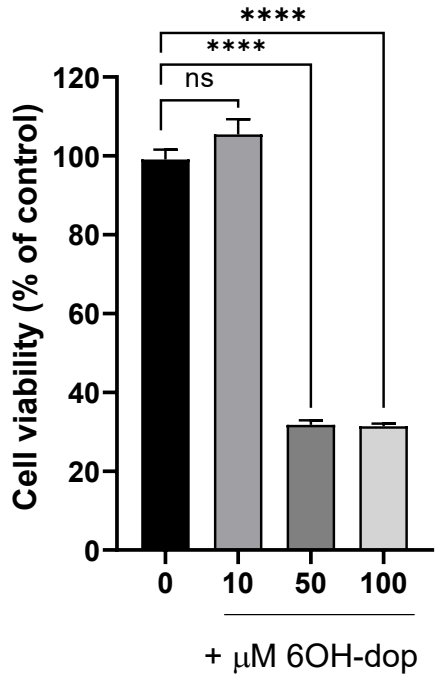

Supplementary figure 4: Cell viability on SHSY-5Y cells after exposure of 6 hydroxydopamine (6OH-dop) for 24 h. ****$p \leq 0.0001$. $n = 9$ in in 3 independent batches and analysed by an one way ANOVA

8. References

1. Winklhofer KF, Haass C. Mitochondrial dysfunction in Parkinson's disease. Biochimica et Biophysica Acta (BBA) - Molecular Basis of Disease. 2010;1802(1):29-44.
2. Park J-S, Davis RL, Sue CM. Mitochondrial Dysfunction in Parkinson's Disease: New Mechanistic Insights and Therapeutic Perspectives. Current Neurology and Neuroscience Reports. 2018;18(5):21.
3. Moore DJ, West AB, Dawson VL, Dawson TM. MOLECULAR PATHOPHYSIOLOGY OF PARKINSON'S DISEASE. 2005;28(1):57-87.
4. Zhang X, Bian J-S. Hydrogen Sulfide: A Neuromodulator and Neuroprotectant in the Central Nervous System. ACS Chemical Neuroscience. 2014;5(10):876-83.
5. Kimura Y, Kimura H. Hydrogen sulfide protects neurons from oxidative stress. 2004;18(10):1165-7.
6. Goubern M, Andriamihaja M, Nübel T, Blachier F, Bouillaud F. Sulfide, the first inorganic substrate for human cells. The FASEB Journal. 2007;21(8):1699-706.
7. Módis K, Coletta C, Erdélyi K, Papapetropoulos A, Szabo C. Intramitochondrial hydrogen sulfide production by 3-mercaptopyruvate sulfurtransferase maintains mitochondrial electron flow and supports cellular bioenergetics. 2013;27(2):601-11.
8. Sanchez-Aranguren L, Marwah MK, Nadeem S. Neuroprotective effects of mitochondrial-targeted hydrogen sulphide donor, AP39 on H2O2-induced oxidative stress in human neuroblastoma SHSY5Y cell line. Advances in Redox Research. 2021;3.
9. Hu LF, Lu M, Tiong CX, Dawe GS, Hu G, Bian JSJAc. Neuroprotective effects of hydrogen sulfide on Parkinson's disease rat models. 2010;9(2):135-46.

10. Hu L-F, Lu M, Wu Z-Y, Wong PT-H, Bian J-SJMp. Hydrogen sulfide inhibits rotenone-induced apoptosis via preservation of mitochondrial function. 2009;75(1):27-34.
11. Tiong CX, Lu M, Bian JSJBjop. Protective effect of hydrogen sulphide against 6-OHDA-induced cell injury in SH-SY5Y cells involves PKC/PI3K/Akt pathway. 2010;161(2):467-80.
12. Zhang X, Bian J-SJAcn. Hydrogen sulfide: a neuromodulator and neuroprotectant in the central nervous system. 2014;5(10):876-83.
13. Szczesny B, Módis K, Yanagi K, Coletta C, Le Trionnaire S, Perry A, et al. AP39, a novel mitochondria-targeted hydrogen sulfide donor, stimulates cellular bioenergetics, exerts cytoprotective effects and protects against the loss of mitochondrial DNA integrity in oxidatively stressed endothelial cells in vitro. 2014;41:120-30.
14. Gerő D, Torregrossa R, Perry A, Waters A, Le-Trionnaire S, Whatmore JL, et al. The novel mitochondria-targeted hydrogen sulfide (H2S) donors AP123 and AP39 protect against hyperglycemic injury in microvascular endothelial cells in vitro. 2016;113:186-98.
15. Pomierny B, Krzyzanowska W, Jurczyk J, Skorkowska A, Strach B, Szafarz M, et al. The Slow-Releasing and Mitochondria-Targeted Hydrogen Sulfide (H(2)S) Delivery Molecule AP39 Induces Brain Tolerance to Ischemia. Int J Mol Sci. 2021;22(15):7816.
16. Zhao F-l, Fang F, Qiao P-f, Yan N, Gao D, Yan Y. AP39, a Mitochondria-Targeted Hydrogen Sulfide Donor, Supports Cellular Bioenergetics and Protects against Alzheimer's Disease by Preserving Mitochondrial Function in APP/PS1 Mice and Neurons. Oxidative Medicine and Cellular Longevity. 2016;2016:8360738.
17. Marwah MK, Shokr H, Sanchez-Aranguren L, Badhan RKS, Wang K, Ahmad S. Transdermal Delivery of a Hydrogen Sulphide Donor, ADT-OH Using Aqueous Gel Formulations for the Treatment of Impaired Vascular Function: an Ex Vivo Study. Pharmaceutical Research. 2022;39(2):341-52.
18. Williams AC, Barry BW. Penetration enhancers. Advanced Drug Delivery Reviews. 2012;64:128-37.
19. Ebrahimzadeh MH, Mousavi SK, Ashraf H, Abubakri R, Birjandinejad A. Transdermal fentanyl patches versus patient-controlled intravenous morphine analgesia for postoperative pain management. Iranian Red Crescent medical journal. 2014;16(5):e11502.
20. Galosi M, Troisi A, Toniolo P, Pennasilico L, Cicirelli V, Palumbo Piccionello A, et al. Comparison of the Transdermal and Intravenous Administration of Buprenorphine in the Management of Intra- and Postoperative Pain in Dogs Undergoing a Unilateral Mastectomy. 2022;12(24):3468.
21. Xie L, Tiong CX, Bian J-SJAJoP-CP. Hydrogen sulfide protects SH-SY5Y cells against 6-hydroxydopamine-induced endoplasmic reticulum stress. 2012;303(1):C81-C91.
22. Marwah M, Badhan RKS, Lowry D. Development of a novel polymer-based carrier for deformable liposomes for the controlled dermal delivery of naringenin. Journal of Liposome Research. 2022;32(2):181-94.
23. Dias HK, Brown CL, Polidori MC, Lip GY, Griffiths HR. LDL-lipids from patients with hypercholesterolaemia and Alzheimer's disease are inflammatory to microvascular endothelial cells: mitigation by statin intervention. Clinical science (London, England : 1979). 2015;129(12):1195-206.
24. Elbakary B, Badhan RKS. A dynamic perfusion based blood-brain barrier model for cytotoxicity testing and drug permeation. Scientific Reports. 2020;10(1):3788.
25. Sanchez-Aranguren LC, Ahmad S, Dias IHK, Alzahrani FA, Rezai H, Wang K, et al. Bioenergetic effects of hydrogen sulfide suppress soluble Flt-1 and soluble endoglin in cystathionine gamma-lyase compromised endothelial cells. Scientific Reports. 2020;10(1):15810.
26. Al-Kinani AA, Zidan G, Elsaid N, Seyfoddin A, Alani AWG, Alany RG. Ophthalmic gels: Past, present and future. Adv Drug Deliv Rev. 2018;126:113-26.
27. Simola N, Morelli M, Carta AR. The 6-hydroxydopamine model of Parkinson's disease. Neurotoxicity research. 2007;11(3-4):151-67.
28. Latchoumycandane C, Anantharam V, Jin H, Kanthasamy A, Kanthasamy A. Dopaminergic neurotoxicant 6-OHDA induces oxidative damage through proteolytic activation of PKCδ in cell

culture and animal models of Parkinson's disease. Toxicology and applied pharmacology. 2011;256(3):314-23.
29. Iglesias-González J, Sánchez-Iglesias S, Méndez-Álvarez E, Rose S, Hikima A, Jenner P, et al. Differential toxicity of 6-hydroxydopamine in SH-SY5Y human neuroblastoma cells and rat brain mitochondria: protective role of catalase and superoxide dismutase. Neurochemical research. 2012;37(10):2150-60.
30. Carrer V, Alonso C, Pont M, Zanuy M, Córdoba M, Espinosa S, et al. Effect of propylene glycol on the skin penetration of drugs. Archives of Dermatological Research. 2020;312(5):337-52.
31. Hoelgaard A, Møllgaard B. Dermal drug delivery — Improvement by choice of vehicle or drug derivative. Journal of Controlled Release. 1985;2:111-20.
32. Ostrenga J, Steinmetz C, Poulsen B, Yett SJJops. Significance of vehicle composition II: prediction of optimal vehicle composition. 1971;60(8):1180-3.
33. Bouwstra J, Peschier L, Brussee J, Boddé HJIjop. Effect of N-alkyl-azocycloheptan-2-ones including azone on the thermal behaviour of human stratum corneum. 1989;52(1):47-54.
34. Zhang Q, Li P, Roberts MSJJocr. Maximum transepidermal flux for similar size phenolic compounds is enhanced by solvent uptake into the skin. 2011;154(1):50-7.
35. Suksaeree J, Simchareon W, Pichayakorn W. Effect of glycols permeation enhancer on the release and permeation of meloxicam-natural rubber film through pig skin. Journal of Drug Delivery Science and Technology. 2021;66.
36. Islam MT, Rodriguez-Hornedo N, Ciotti S, Ackermann CJPr. Rheological characterization of topical carbomer gels neutralized to different pH. 2004;21(7):1192-9.
37. Hurler J, Engesland A, Poorahmary Kermany B, Škalko-Basnet N. Improved texture analysis for hydrogel characterization: Gel cohesiveness, adhesiveness, and hardness. 2012;125(1):180-8.
38. Al-Kassas R, Wen J, Cheng AE, Kim AM, Liu SSM, Yu J. Transdermal delivery of propranolol hydrochloride through chitosan nanoparticles dispersed in mucoadhesive gel. Carbohydr Polym. 2016;153:176-86.
39. Hurler J, Engesland A, Poorahmary Kermany B, Škalko-Basnet NJJoAPS. Improved texture analysis for hydrogel characterization: Gel cohesiveness, adhesiveness, and hardness. 2012;125(1):180-8.
40. Ma D, Djemai A, Gendron CM, Xi H, Smith M, Kogan J, et al. Development of a HPMC-based controlled release formulation with hot melt extrusion (HME). Drug Dev Ind Pharm. 2013;39(7):1070-83.
41. YILMAZER G, CARRILLO AR, KOKINI JL. Effect of Propylene Glycol Alginate and Xanthan Gum on Stability of O/W Emulsions. 1991;56(2):513-7.
42. Higuchi TJJSCC. Physical chemical analysis of percutaneous absorption process from creams and ointments. 1960;11:85-97.
43. Barry BWJJocr. Mode of action of penetration enhancers in human skin. 1987;6(1):85-97.
44. Karakatsani M, Dedhiya M, Plakogiannis FM. The effect of permeation enhancers on the viscosity and the release profile of transdermal hydroxypropyl methylcellulose gel formulations containing diltiazem HCl. Drug Development and Industrial Pharmacy. 2010;36(10):1195-206.
45. Temsamani J, Scherrmann J-M, Rees AR, Kaczorek M. Brain drug delivery technologies: novel approaches for transporting therapeutics. Pharmaceutical science & technology today. 2000;3(5):155-62.
46. Ikeda K, Marutani E, Hirai S, Wood ME, Whiteman M, Ichinose F. Mitochondria-targeted hydrogen sulfide donor AP39 improves neurological outcomes after cardiac arrest in mice. Nitric Oxide. 2015;49:90-6.
47. Ikeda K, Marutani E, Hirai S, Wood ME, Whiteman M, Ichinose F. Mitochondria-targeted hydrogen sulfide donor AP39 improves neurological outcomes after cardiac arrest in mice. Nitric Oxide. 2015;49:90-6.